Research Article

Galectin-3 expression and secretion by tumor-associated macrophages in hypoxia promotes breast cancer progression

Lei Wang[1], Ying-ShuangLi[1], Lu-Gang Yu[2], Xin-Ke Zhang[1], Lin Zhao[1], Fu-Lian Gong[1,3], Xiao-Xia Yang[1], Xiu-Li Guo[1]*

[1]Department of Pharmacology, Key Laboratory of Chemical Biology (Ministry of Education), School of Pharmaceutical Sciences, Shandong University, Jinan, 250012, China.

[2]Department of Cellular and Molecular Physiology, Institute of Translational Medicine, University of Liverpool, Liverpool, UK.

[3]Department of Pharmacy, Tianjin Children's Hospital, Tianjin, China.

*Correspondence should be addressed to

Xiu-Li Guo,

Department of Pharmacology, School of Pharmaceutical Sciences, Shandong University, No. 44 Wen Hua Xi Road, Jinan 250012, P.R. China.

E-mail:guoxl@sdu.edu.cn (X.L.G)

Fax: +86-531-88382490

Telephone: +86-531-88382490

Abstract

Tumor-associated macrophages (TAMs) have been shown to be associated with poor prognosis of cancer and are predominately localized in the hypoxia regions of tumor. We demonstrated in this study that hypoxia increases the synthesis and secretion of galectin-3 by TAMs. The increased expression of galectin-3 in TAMs was seen to be associated with nucleation of transcription factor NF-κB through generation and activation of ROS and promoted tumor growth and metastasis *in vitro* and in mice through multiple molecular mechanisms. It was found that the TAMs-mediated promotion of tumor growth and metastasis in hypoxia was inhibited by administration of macrophage-depletion agent clodronate liposomal (CL) or galectin-3 inhibitor modified citric pectin (MCP) in orthotopic syngeneic mammary adenocarcinoma model and metastasis model. Co-administration of anti-angiogenesis agent sorafenib or bevacizumab with CL and MCP showed to cause stronger inhibition of tumor growth and metastasis than administration of each agent alone. These results indicate that hypoxia-induced galectin-3 expression and secretion from TAMs promotes tumor growth and metastasis. Targeting the actions of galectin-3 in hypoxia may be a potential therapeutic strategy for cancer treatment.

Keywords: TAMs; hypoxia; galectin-3; bevacizumab; modified citrus pectin

1. Introduction

The presence of large quantities of tumor-associated macrophages (TAMs) in cancer is often associated with increased levels of tumor angiogenesis, metastasis and poor prognosis[1]. TAMs are frequently seen in the hypoxic regions of the tumors where they have been speculated to acquire and exert tumor-promoting actions[2].

Galectin-3 is a family member of the β-galactoside binding proteins which share similar carbohydrate-recognition domains. It is a multifunctional protein and is involved in many aspects of macrophage activity, such as migration, apoptosis, phagocytosis, and adhesion[3] [4-6]. Galectin-3 is expressed in the cytoplasm and nucleus and is also secreted outside the cells[7, 8]. Intracellular galectin-3 participates in cell proliferation, differentiation, and apoptosis while extracellular galectin-3 mediates cell-cell and cell-environment interactions. Expression of galectin-3 is commonly increased in inflammation, cancer and a few other diseases such as heart failure and is closely involved in tumor cell transformation, migration, invasion and metastasis[8-10].

Galectin-3 is known to be secreted by epithelial and immune cells[11, 12] and its expression has been reported to be particularly high in the hypoxic regions in breast, lung and prostate cancer[4-6]. However, the relationship between galectin-3 and hypoxic TAMs, and the impact of this relationship on the tumor development and metastasis are unclear. It was found in this study that galectin-3 expression and secretion was significantly increased in TAMs in hypoxia and promoted cancer cell migration and invasion *in vitro* and TAMs-mediated metastasis *in vivo* and such effect was inhibited by the presence of galectin-3 inhibitors.

2. Materials and methods

2.1 Reagents

β-lactose and metformin were purchased from Sigma (Darmstadt, Germany). MCP was purchased from Econugenics (Santa Rosa, USA). Compound C, AICAR, Ly294002 and 2ME2 were the products of Selleck (Shanghai, China). PDTC, NAC and rosup were purchased from Beyotime (Haimen, China). Sorafenib was purchased from Hiboled century biotechnology (Shenzhen, China). Liposomal clodronate was purchased from YEASEN (Amsterdam, Netherlands). Bevacizumab was purchased from Roche (Basel, Switzerland).

2.2 Cell lines

Human monocyte (THP-1), Human breast cancer cell line (MDA-MB-231), Human umbilical vein endothelial cells (HUVECs) were obtained from Type Culture Collection of the Chinese Academy of Sciences, Shanghai, China. Luciferase-labeled MDA-MB-231 cells (MDA-MB-231-luc cells) and 4T1cells (4T1-luc cells) which were kindly provided by Caliper Life Sciences, Inc (Hopkinton, MA, USA). All cells were cultured in RPMI-1640medium supplemented with 10% fetal bovine serum (Gibico, CA, USA) at 37 ℃, 5% CO_2.

2.3 Preparation of condition medium

Cells were cultured in serum-free 1640 medium for 48 h. The culture medium was collected and centrifuged at 1000×g for 5 min. The supernatant was taken as initial condition medium (iCM). Thirty percent (v/v) fresh complete medium was added to iCM prior to the experiments to replenish the consumption of nutrition to obtain the final CM.

2.4 Preparation of M2 phenotype macrophage (M2) or TAMs

For the preparation of M2 type macrophages, THP-1 cells (1×10^5 cells per well) seeded in

24-well plates were treated with 320 nM PMA (Sigma, Darmstadt, Germany) for 24 h at 37°C, followed by incubation with 20 ng/mL IL-4 (Petprotec, RockyHill, NJ) and 20 ng/mL IL-13 (Petprotec, RockyHill, NJ) for an additional 72 h at 37°C to obtain M2 type macrophages.

For the preparation of TAMs, THP-1 cells (1×10^5 cells per well) seeded in 24-well plates were treated with 320 nM PMA for 24 h at 37°C, followed by incubation with CM of MDA-MB-231 cells for an additional 72 h at 37°C.

2.5 Establishment of hypoxia model

Chemical hypoxia cellular model was established by added chemical regent $Na_2S_2O_4$ at 1~8 mM (Sigma, Darmstadt, Germany) into the medium for 1 h before other treatment on cells. Physical hypoxia model was accomplished by using hypoxia chambers. The hypoxia chamber used for the cell experiments is the ProOX C21 and for animal experiments is ProOX 360 of BioSpherix Ltd. (Redfield, NY, USA).

2.6 Identification of M2 or TAMs by flow cytometry

The above prepared macrophages were collected with a scraper and blocked with 3% BSA for 45 min, and then were incubated with PE-conjugated anti-human CD163 antibodies (333605; Biolegend, California, USA) for 45 min or FITC-conjugated anti-human CD68 antibodies (333805; Biolegend, California, USA) according to the manufacturers' instructions. At least 1×10^4 cells of each sample were analyzed using the BD FACS Calibur cytometer (Becton Dickinson, CA, USA).

2.7 Cell transfection

Cell transfections were carried out with the Micropoly-transfecter Cell Reagent (Micropoly, Shanghai, China) according to the manufacturer's instructions. The coding strand targeting by galectin-3 siRNA duplex was 5'-CAC GCT TCA ATG AGA ACA ACA-3'. The sequence of

control siRNA was 5'- TTC TCC GAA CGT GCT GTC TTT-3'.

2.8 *In vitro* angiogenesis assay

One hundred microliter Matrigel (BD Biosciences, MA, USA) was added into pre-cooled 96-well plates on ice and incubated for 30 min at 37 °C. HUVECs (3×10^4 cells per well) were added into the 96-well plate and cultured with 100 μL CM for 6 h at 37 °C before visualization and image under a light microscope. Photographs were captured with a Nikon inverted microscope (Nikon, Tokyo, Japan), and the length of tubes was counted and analyzed.

2.9 *In vitro* vascular mimicry assay

Nanty-six-well plates were precoated with 100 μL BD Matrigel. MDA-MB-231 cells (3×10^4 cells per well) were added and cultured with 100 μL CM for 6 h at 37 °C. Tube formation of vascular mimicry was visualized under a light microscope. Photographs were captured with a Nikon inverted microscope (Nikon, Tokyo, Japan), and the length of tubes was counted and analyzed.

2.10 MTT assay

Cell proliferation was determined by 3-(4,5-Dimethylthiazol-2-yl)-2,5- diphenyltetrazolium bromide (MTT; Solarbio, Beijing, China) assay. The cells (4×10^3 cells per well) were seeded on 96-well plates and cultured for 24 h, then 100 μL of CM of TAMs was added and incubated for 48 h before 20 μL of MTT solution (5 mg/mL in phosphate buffered saline; PBS) was added for further 4 h. The medium was removed and replaced with 150 μL of DMSO to dissolve the formazan crystal. The absorbance was measured at 570 nm using Thermo Multiskan GO microplate reader (Thermo-1510, CA, USA).

2.11 Transwell co-culture system

THP-1 cells (1×10^5cells per well) seeded in 24-well plates were differentiated into M2 or TAMs as described above. For invasion assay, the upper chamber was first coated with Matrigel. For migration assay, no Matrigel was added to the upper chamber. MDA-MB-231 cells were delivered into the upper compartment of transwell chamber (Corning, NY, USA) and co-cultured with TAMs in the lower compartment. After 48h, the cells remained on the upper surface of the transwell chamber were removed by cotton swabs. Cells on the bottom side of the transwell chamber were fixed by cold methanol-glacial acetic acid and stained with crystal violet, and counted.

2.12 Western blot analysis

The cells were lysed in RIPA buffer and the protein concentration was determined with the BCA protein assay. Equal amounts of protein were separated by sodium dodecyl sulphate polyacrylamide gel electrophoresis (SDS-PAGE) and transferred onto a polyvinylidene fluoride (PVDF) membrane (Millipore, Billerica, USA). The membranes were washed, blocked with TBST buffer (20 mM Tris-buffered saline and 0.1% Tween-20) containing 5% (w/v) nonfat dry milk overnight before incubated with antibodies against human PI3K (#4255), HIF-1α (#36169), NF-κB (#4764) p-AMPK (#2537, Cell Signaling Technology, CST, Boston, MA, USA), AMPK (10929-2-AP, Proteintech, Wuhan, China) and anti-β-actin (ZF-0313, ZS Bio. Beijing, China). The secondary antibodies used were either goat anti-mouse or goat anti-rabbit IgG (PIERCE, 1:10000 in TBST), depending on the primary antibody. Antibody bindings were detected by enhanced chemiluminescence reagent and quantified by densitometry using a ChemiDoc XRS + molecular imager (Bio-Rad, CA, USA).

2.13 Quantitative real-time PCR

Total RNA was extracted from the cell pellets using TRIzol Reagent (Invitrogen California,

USA) following the manufacturer's instructions. First-strand cDNA was produced from total RNA by using a qPCR RT Kit (Toyobo, Osaka, Japan), according to manufacturer's instructions. Samples were cycled for 30 s at 95°C, 30 s at 59°C and 30 s for 72°C for 40 cycles. QRT-PCR of the mRNA was performed on a LightCycler480 II real-time PCR system (Roche, Basel, Switzerland), using the SYBR-Green Chemistry (Toyobo, Osaka, Japan). Detail information of the primers sequences as below: galectin-3 sequence (5'-3'): ATGCAAACAGAATTGCTTTAG ATT; IL-10 sequence (5'-3'): TCTCCGAGATGCCTTCAGCAGA; IL-12 sequence (5'-3'): GACATTCTGCGTTCAGGTCCAG; NOS2sequence (5'-3'): GCTCTAC ACCTCCAATGTGACC.

2.14 Immunofluorescence staining

THP-1 cells (1×10^5 cells per well) seeded in 24-well plates with a coverslip/well were differentiated as described above. The cells were fixed in 4% paraformaldehyde in PBS at room temperature for 20 min, and permeabilized for 30 min in PBS containing 0.2% Triton X-100 (Beyotime, Haimen, China), 10% BSA (Sigma, Darmstadt, Germany) and primary antibodies at 4°C overnight. Then cells were washed three times with PBST and incubated at room temperature for 1 h with anti-rabbit or anti-mouse secondary antibodies. Finally, cells were labeled with Hoechst 33342 to stain the nucleus, and fluorescence images were taken with fluorescence microscope (NIKON Ti-U, Nikon, Japan).

2.15 ELISA

After transfection with siGal-3, the cells were cultured in serum-free 1640 medium for 24 h. The supernatant of the culture medium was collected, centrifuged at 1000× g for 5 min, and stored at -20 ℃. The galectin-3 and VEGFA in culture supernatants were assessed separately

using Quantikine ELISA kits (R&D Systems, MN, USA) according to the manufacturer's instructions.

2.16 Glucose consumption assay

Glucose level in culture medium supernatant of TAMs was detected using Glucose Assay Kit (Nanjing Jiancheng Bioengineering Institute, Nanjing, China). Glucose intake by TAMs is equal to the amount of glucose in fresh medium minus the amount of glucose in the supernatant of treatment group. Cells were collected and the number of cells was counted by cell counter. The values of glucose level were normalized to the number of cells.

2.17 Mouse metastasis model and IVIS imaging

Five-week-old female Balb/c mice and Balb/c nude mice were purchased from the Animal Center of China Academy of Medical Science (Beijing, China) and housed under pathogen-free conditions. All animal experiment protocols were conducted in strict accordance with the Institutional Guidelines of Animal Care and Use Committee of Shandong University.

In the 4T1-luc orthotopic syngeneic tumor mouse model, fifty Balb/c mice were injected with 5×10^5 4T1-luc cells into the mammary fat pad under #3 mammary gland. Once the tumor volume reached 100 ~ 200 mm^3, over-or under-sized mice were excluded. There remaining mice were divided randomly into four groups (n = 5) for effect of galectin-3 inhibitor MCP or CL (to induce monocyte depletion) on orthotopic growth of breast cancer in hypoxia: normaxia control (normal saline, i.g.); hypoxia control (8% O_2 condition 6 h/day); hypoxia (8% O_2 condition 6 h/day) + MCP (0.5 μL/g/day, i.t.); hypoxia (8% O_2 condition 6 h/day) + CL (10 μL/g/week, i.v.). Other remaining mice were randomly divided into four groups for effect of bevacizumab and MCP on orthotopic growth of breast cancer: control (normal saline, i.g.); MCP (0.5 μL/g/day, i.t.); bevacizumab (5 mg/kg/week, i.v.); MCP (0.5 μL/g/day, i.t.) +

bevacizumab (5 mg/kg/week, i.v.). The body weight and tumor volume of all animals were measured every 3 days. $V = L \times W^2/2$ and was used to calculate the tumor volume (V), in which W refers to the short axis and L refers to the long axis.

In the metastasis model: nude mice were intravenous injected with 1×10^5 MDA-MB-231-luc cells by tail vein. Mice were randomly divided into five groups (n = 5): control; metastasis model (normal saline, i.g.); sorafenib (15 mg/kg/day, i.g.); CL (10 μL/g/week, i.v.); sorafenib (15 mg/kg/day, i.g.) + CL (10 μL/g/week, i.v.). The body weights of all of the animals were measured every 3 days.

The mice were anesthetized by isoflurane and imaged using the IVIS Kinetic *in vivo* imaging system (Caliper Life Sciences, MA, USA) at nine minutes after injecting D-luciferin potassium salt intraperitoneally every 7 days for up to 21 days. At the end of the experiment, the mice were sacrificed, and the xenografts and lungs were removed and weighed.

2.18 Immunohistochemical assay

Tumors or lung tissues of the metastasis mice were dissected and directly embedded in O.C.T. compound. Sections were cut and fixed with cold 4% paraformaldehyde, immunostained with mouse anti-galectin-3 (1:200; 60207-1, Proteintech, Wuhan, China), rabbit anti-CD31 (1:100; #3529, CST, Boston, MA), rabbit anti-CD68 (1:50, #76437, CST, Boston, MA) and Hypoxyprobe-1 (1:100; Hypoxyprobe Inc., Burlington, MA) antibodies. Rabbit anti-mouse rhodamine antibody (1:200; Santa Cruz, CA, USA) or rabbit anti- mouse FITC antibody (1:200; Santa Cruz, CA, USA) were applied as secondary antibodies. Sections were incubated with DAPI (Solarbio, Beijing, China) for 5 min at room temperature. The immunofluorescence intensity was observed by fluorescence microscope (NIKON Ti-U, Nikon, Japan).

2.19 Statistical analysis

All quantitative data are expressed as mean ± SD. Multiple comparisons were performed by one-way analysis of variance (one-way ANOVA). A P-value < 0.05 was considered statistically significant. Statistical analysis was performed using the SPSS/Win 13.0 software.

3. Results

3.1 TAMs promote proliferation, invasion and migration of MDA-MB-231 cells, and angiogenesis of HUVECs under hypoxia

Human monocyte cell line THP-1 is widely used as a model for monocyte/macrophages differentiation. M2-polarised macrophages (M2) were obtained from THP-1 cells after treatment with IL-4 and IL-13. TAMs were obtained from incubation of THP-1 cells with conditioned cell culture medium (CM) from human breast cancer MDA-MB-231 cells. As shown in Fig. 1A, the resulting TAMs exhibited a significantly higher level of M2-specific cell-surface markers CD68 and CD163 compared with THP-1 cells. At mRNA level, the expressions of M2 markers, IL-1Rα and IL-10, were both significantly upregulated while the expression of M1 macrophage markers NOS2 and IL-12 were both downregulated in the TAMs (Fig. 1B). These confirm the successful differentiation of THP-1 monocytes into M2-polarized TAMs by CM of MDA-MB-231 cells.

Treatment with CM of both M2 and TAMs showed to have increased the ability of HUVECs to form micro-tube structures in hypoxia (Fig. 1C), and also increased MDA-MB-231 cells proliferation (Fig. 1D). Co-culture of M2 or TAMs with MDA-MB-231 cells also enhanced MDA-MB-231 cell migration and invasion in trans-wells under hypoxia (Fig. 1E). These findings suggest that the presence of TAMs promotes proliferation, invasion and migration of breast cancer cells, and also enhances angiogenesis under hypoxia.

3.2 Hypoxia induces the expression and secretion of galectin-3 by TAMs

Under hypoxia conditions of either culturing cells in hypoxic chambers (1% O_2) or by exposing cells to sodium dithionite ($Na_2S_2O_4$), the expression of galectin-3 in M2 and TAMs at protein (Fig. 2A) and mRNA levels (Fig. 2B), as well as galectin-3 secretion (Fig. 2C) by M2 or TAMs, were all significantly increased in hypoxic degree- and time-dependent manners. A general increase of galectin-3 translocation from the cytoplasm to the nucleus in TAMs was also observed under hypoxia (Fig. 2D). In the 4T1-luc orthotopic syngeneic breast cancer mouse model, galectin-3 was seen to be highly expressed in the hypoxic (hypoxiprobe-1 positive) regions in the tumor (Fig. 2E). These findings indicate that hypoxia induces TAMs expression and secretion of galectin-3.

3.3 TAMs-mediated expression and secretion of galectin-3 under hypoxia promote migration/invasion of breast cancer cells

To determine the role of the increased galectin-3 secretion by TAMs or increased expression of galectin-3 in TAMs in TAMs-mediated promotion of tumor cell migration and invasion, the migration and invasion of MDA-MB-231 cells were assessed by siRNA (siGal-3) galectin-3 suppression in TAMs and the presence of galectin-3 binding inhibitor, β-lactose. Suppression of galectin-3 expression by siGal-3 in M2 or TAMs or treatment with β-lactose of M2 (Fig. 3A) or TAMs (Fig. 3B) reduced migration and invasion of MDA-MB-231 cell in hypoxia in co-culture of M2 or TAMs with MDA-MB-231 cells. The presence of modified citric pectin (MCP), another galectin-3 inhibitor, in the co-culture also reduced TAMs-mediated promotion of MDA-MB-231 cells migration and invasion (Fig. 3C). The inhibitory effect of siGal-3 in TAMs on

MDA-MB-231 cell migration and invasion was lower in normoxia than that in hypoxia (Fig. 3D). In addition, suppression of galectin-3 by siGal-3 in M2 or TAMs obviously reduced the proliferation of MDA-MB-231 cells by incubation with CM of M2 or TAMs in hypoxia in comparison to scramble siRNA control group (Fig. 3E), which suggest that the hypoxia-induced galectin-3 in TAMs may also be involved in the promotion of MDA-MB-231 cells proliferation. These results indicate that under hypoxia, TAMs-associated galectin-3 expression and secretion of galectin-3 are both involved in TAMs-mediated promotion of tumor cell proliferation and migration/invasion.

Moreover, suppression of galectin-3 expression by siGal-3 in M2 or TAMs caused a reduction of cell survival with the inhibition rate of 9.6 % or 8.57 %, respectively (Fig. 3F), which indicated that the inhibition of TAMs survival had a limited contribution to the inhibitory effects of siGal-3 on the migration/invasion of MDA-MB-231 cells. Suppression of galectin-3 expression caused a significant reduction on glucose consumption of M2 or TAMs in hypoxia (Fig. 3G). The ELISA result showed that suppression of intracellular galectin-3 expression also decreased the secretion of galectin-3 (Fig. 3H) and vascular endothelial growth factor A (VEGFA) (Fig. 3I) from both M2 and TAMs. These results indicate that an increased uptake of glucose and increase of VEGFA secretion by TAMs, caused by hypoxia-induced expression of galectin-3 in TAMs, may contribute to TAMs-mediated promotion of angiogenesis.

3.4 Galectin-3 secretion by TAMs promotes angiogenesis and vascular mimicry under hypoxia

To investigate whether galectin-3 expression and secretion by TAMs were involved in TAMs-mediated effect, HUVECs tube formation and vascular mimicry (VM) of MDA-MB-231 cells

was assessed with and without galectin-3 suppression and in the presence or absence of lactose under hypoxia. Suppression of galectin-3 expression in TAMs or presence of lactose resulted in significant increase of VM formation of MDA-MB-231 cells as well as significant increase of HUVECs tube formation (Fig. 4A and 4B). The presence of lactose and siRNA galectin-3 knockdown in combination showed to cause a bigger effect than the presence of lactose or galectin-3 knockdown alone. The siGal-3 in TAMs also showed a similar inhibitory effect to tube formation and VM formation in normoxia but to a less degree than under hypoxia (Fig. 4C). Treatment of the cells with MCP reduced the pro-angiogenesis effects of TAMs (Fig. 4D). A less inhibitory effect on HUVECs proliferation was observed from CM of TAMs treated with siGal-3 than the scramble siRNA control group and this inhibitory effect of siGal-3 occurred less in normoxia than in hypoxia (Fig. 4E). siGal-3 or β-lactose, alone or in combination, inhibited invasion and migration of HUVECs co-cultured with TAMs in hypoxia (Fig. 4F). These indicate that both intracellular and extracellular galectin-3 in hypoxic TAMs are involved in TAMs-mediated promotion of angiogenesis.

3.5 Upregulation of galectin-3 in TAMs under hypoxia is dependent on NF-κB via ROS

To investigate the mechanism of galectin-3 upregulation in TAMs under hypoxia, expression and activation of several cell signaling proteins in TAMs in hypoxia were examined. Twenty-four hours treatment of TAMs under hypoxia caused the increase of adenosine 5‘-monophosphate-activated protein kinase (p-AMPK), PI3K, phosphorylated AKT, hypoxia inducible factor-1α (HIF-1α) and intranuclear transfer of nuclear factor kappa-B (NF-κB) (Fig. 5A and 5B). The presence of AMPK inhibitor compound C or PI3K inhibitor LY294002 prevented the upregulation of galectin-3 in TAMs under hypoxia, but not under normoxic condition. The presence of NF-κB inhibitor PDTC dramatically reduced the galectin-3

expression under both normoxia and hypoxia. Interestingly, the presence of HIF-1α inhibitor 2ME2 increased the expression of galectin-3 in normoxia but not in hypoxia (Fig. 5C). Together, these results suggest that upregulation of galectin-3 in TAMs in hypoxia likely involves in activation of AMPK, PI3K and NF-κB signaling pathways.

The involvement of AMPK activation in the regulation of galectin-3 expression seems to be supported by the discovery that the presence of AMPK activator, AICAR, promoted galectin-3 expression in TAMs in normoxia (Fig. 5D). However, the presence of another AMPK activator metformin suppressed galectin-3 expression in TAMs in hypoxia (Fig. 5E), to the same extent as AMPK inhibitor compound C (Fig. 5D and 5E). This suggests the involvement of AMPK in the regulation of TAMs-mediated galectin-3 expression in hypoxia may be complex. Giving the opposite effects of AICAR and metformin have been shown previously to regulate intracellular reactive oxygen species (ROS) level[13, 14], ROS might be involved in the complex actions of AMPK in regulation of galectin-3 expression in hypoxic TAMs.

To test this possibility, ROS levels in TAMs were analyzed. It was found that hypoxic treatment led to a dramatic increase of ROS in TAMs which was inhibited by the presence of compound C, LY294002, and PDTC. The presence of HIF-1α inhibitor 2ME2 increased the ROS level in normoxia but not in hypoxia (Fig. 5F). The changes of these inhibitors on the ROS level in TAMs were paralleled with the changes of galectin-3 levels (Fig. 5C). This suggested that the ROS may indeed be involved in the regulation of galectin-3 expression in TAMs in hypoxia. This conclusion was supported by the discoveries that treatment on TAMs with pro-oxidant rosup in normoxia increased galectin-3 expression while treatment with ROS inhibitor NAC downregulated galectin-3 expression, and treatment with NAC reduced the increase of galectin-3 expression induced by 2ME2 (Fig. 5G).

As NF-κB was shown to be altered in hypoxic TAM (Fig. 5B), we then investigated the

relationship of ROS on galectin-3 with NF-κB expression. The presence of compound C, LY294002, PDTC and NAC, which could all inhibit ROS generation in hypoxic TAMs, reduced the increase of NF-κB expression in TAMs caused by hypoxia. HIF-1α inhibitor 2ME2 increased NF-κB of TAMs in normaxia. And NAC reduced the upregulation of NF-κB by 2ME2 in normaxia (Fig. 5H). The effects of these inhibitors on NF-κB level were paralleled with the changes of galectin-3 mRNA expression. These findings indicate that ROS-associated upregulation of galectin-3 expression in TAMs under hypoxia is related to nuclear accumulation of NF-κB.

3.6 Hypoxia-induced galectin-3 secretion promotes tumor metastasis and angiogenesis *in vivo*

The effect of hypoxia on galectin-3expression in TAMs was further assessed *in vivo* in a 4T1-luc orthotopic syngeneic mouse model of mammary adenocarcinoma. After 21 consecutive treatments with 8% O_2 for 6 h/day (hypoxia group), the expressions of CD68 (M2 marker) and galectin-3 in tumor tissue were significantly increased in comparison to that in the control mice treated with 21% O_2 (normoxia control group) (Fig. 6A), indicating that hypoxia induces macrophage tumor infiltration and galectin-3 secretion. It was found that the expression of CD31 (vascular endothelial cell marker) in tumor were also significantly increased in the hypoxia group (mice exposure to 8% O_2) in comparison to the normoxia group (exposure to 21% O_2) (Fig. 6B), suggesting increased of angiogenesis.

Lung metastasis of 4T1-luc cells from mammary fat pad was significantly higher in the hypoxia group than in the normoxia group assessed by an *in vivo* imaging system (Fig. 6C). Intratumoral injection (i.t) of 2% (0.5 μL/g/day) MCP for 21 days dramatically inhibited lung

metastasis of 4T1-luc cells and reduced the CD31 expression (Fig. 6B and 6C). Administration of liposomal clodronate (CL), which can deplete the macrophage[15], also inhibited the lung metastasis of 4T1-luc cells. The level of serum galectin-3 in the hypoxia group was significantly higher in comparison to the normaxia group (Fig. 6D). Administration of MCP or liposomal clodronate both reduced the serum galectin-3 level in the hypoxic mice. Together, these results suggest that hypoxia promotes TAMs tumor infiltration and secretion of galectin-3 and increases metastasis of breast cancer.

3.7 Galectin-3 involves in the hypoxia aggravation and macrophage infiltration induced by antiangiogenic agents

It has been reported that the antiangiogenic drug sorafenib promotes infiltration of TAMs, and its combination use with macrophage-depletion agent CL, can synergistically inhibit angiogenesis and lung metastasis[14]. We found that administration of sorafenib (15 mg/kg/day) for 3 weeks significantly reduced lung metastasis of breast cancer MDA-MB-231-luc cells in nude mice. Administration of CL (10 μL/g/weeks) with sorafenib significantly enhanced the inhibitory effects of sorafenib on tumor metastasis (Fig. 7A). Moreover, the serum level of galectin-3 in sorafenib treated group was significantly elevated in comparison to control group, which was reduced when sorafenib was used together with CL (Fig. 7B). These results indicate that the galectin-3 expression may also play an important role in the hypoxia aggravation of tumors under antiangiogenic drug treatment.

Effect of bevacizumab, another antiangiogenic agent that has been reported to aggravate hypoxia and promote macrophage infiltration in tumor[16], was also assessed on galectin-3 expression and TAMs in a 4T1-luc orthotopic syngeneic mouse model. Administration of

bevacizumab (5 mg/kg/week) with MCP (0.5 μL/g/day) for 3 weeks significantly enhanced the inhibitory effects of bevacizumab on tumor progression (Fig. 7C, 7D and 7F) and markedly decreased lung metastasis compared with mice treated with bevacizumab alone (Fig. 7G). Application of bevacizumab induced a significant increase of hypoxic area (evident of hypoxyprobe-1 expression) and intratumoral infiltration (CD68 expression) of TAMs (Fig. 7H), accompanied with an elevation of galectin-3 expression (Fig. 7I). Bevacizumab in combination with MCP also reduced angiogenesis (revealed by an increase of CD31) in mice (Fig. 7J). Moreover, serum level of galectin-3 in the bevacizumab treated mice was significantly elevated in comparison to that in the control mice, which was inhibited in the group with bevacizumab and MCP (Fig.7E). These results indicate the bevacizumab-induced increase of hypoxia and macrophages tumor infiltration was associated with the upregulation of galecin-3 expression.

4. Discussion

Recently, TAMs has drawn significant attention as a potential cancer therapeutic target. However, current TAMs-targeted therapies have not yet been widely accepted in clinical practice because of severe adverse reaction or low specificity[17]. Further development in this area may require new molecular targets. The report in this study showed that macrophages treated by IL-4/IL-13 or by CM from MDA-MB-231 cells both lead macrophages differentiation into M2 type and promote proliferation, invasion migration and angiogenesis of human breast cancer MDA-MB-231 cells under hypoxia *in vitro* and *in vivo*. These effects were shown to be closely linked with upregulation of galectin-3 expression and secretion by TAMs.

It was found in this study that the presence of galectin-3 inhibitors lactose or MCP, or siRNA suppression of galectin-3 expression in TAMs could all inhibit TAMs-mediated promotion of the tumor cell behaviors in hypoxia. This indicates that both extracellular and intracellular galectin-3 are possibly involved in TAM-mediated actions. These discoveries are in keeping

with early studies showing galectin-3 upregulation during progression of prostate carcinoma, endometrial cancer, and colon cancer[18] and promoted tumor cell migration and angiogenesis[6, 19]. Interestingly, galectin-3 in hypoxia was also seen to enhance VEGFA secretion and glucose consumption in TAMs. This suggests that TAMs-associated increase of galectin-3 expression in hypoxia may play a role in TAMs metabolic reprogram, consequently altering TAMs functional phenotypes, such as polarization, secretion ability.

It was found here that the expression of NF-κB, HIF-1α, AMPK and PI3K/AKT signaling were altered in TAMs in response to hypoxia. Change of these signaling proteins and a few others such as p53, homeodomain-interacting protein kinase 2, runt-related protein family and PI3K signaling pathways, have been reported previously to be associated with galectin-3 expression[20, 21]. We observed in this study that the expression or phosphorylation of NF-κB, HIF-1α, AMPK and PI3K in TAMs and TAMs-associated galectin-3 expression was increased under hypoxia, and these changes were inhibited by inhibitors to NF-κB, AMPK, and PI3K and was correlated with changes of intracellular ROS levels.

ROS, generated by Mitochondria in response to cellular stress such as hypoxia, acts as a second messenger to mediate cell actions, including promotion of cell survival, shifting metabolism to increased glycolysis, and activating angiogenesis, etc. by triggering downstream transcriptional signals[22, 23]. The present study showed that the presence of ROS inhibitors compound C, LY294002, PDTC and 2ME2 inhibited ROS production and downregulated galectin-3 expression of TAMs. This suggests a possible link between ROS production and galectin-3 expression in TAMs in hypoxia. Early studies have reported that hypoxia induces ROS production, leading to the stabilization of transcription factors HIF-1α and NF-κB nucleation in macrophage[24, 25]. Both HIF-1α and NF-κB transcription factors are reported to be associated with cellular galectin-3 expression[26, 27]. This suggests that ROS may

participate in the regulation of galectin-3 transcription through activating HIF-1α or NF-κB. However, although HIF-1α expression was elevated in hypoxic TAMs, HIF-1α inhibitor 2ME2 did not show any effect on galectin-3 expression in hypoxia. It instead increased galectin-3 expression in normoxia, which correlated with changes of intracellular ROS levels. Early studies have reported that hybrid glioma cells treated with hypoxia did not affect galectin-3 expression with or without HIF-1α inhibitor (2ME2), although HIF-1α accumulated in the cell nuclei[28]. Based on these early studies and our observation in this study, we deduce that HIF-1α may not be a transcription factor involved in galectin-3 expression in hypoxic TAMs.

The fact that NF-κB nucleation was induced in TAMs by hypoxia and the effects of inhibitors (including compound C, LY29002, 2ME2, rosup and NAC) on NF-κB were paralleled by the above changes of the mRNA expression of galectin-3 indicates that NF-κB is critically involved at transcription level in galectin-3 expression in TAMs in hypoxia, possibly through ROS generation.

In our *in vivo* 4T1-luc orthotopic syngeneic mouse model of mammary adenocarcinoma and tail vein injection of MDA-MB-231 cells metastasis model, hypoxia showed to enhance TAMs tumor infiltration and galectin-3 expression, leading to increased metastasis. This metastasis-promoting effect could be inhibited by administration of galectin-3 inhibitor MCP or macrophage depletion-agent clodronate-liposome (CL). MCP is a group of polysaccharides produced from citrus pectin. It is an effective galectin-3 inhibitor and showed in several early studies to effectively inhibit galectin-3-mediated tumor growth and metastasis, *in vitro* and/or *in vivo*, of prostate carcinoma, colon carcinoma, breast carcinoma, melanoma, multiple myeloma, and hemangiosarcoma[29, 30]. CL is commonly used to eliminate macrophage populations. Early studies have reported that depletion of macrophages by CL significantly enhanced the inhibitory effects of the anti-angiogenesis agent sorafenib on angiogenesis and

lung metastasis of liver cancer[31]. It was found in this study that the growth inhibition and galectin-3 secretion produced by the anti-angiogenesis agents sorafenib or bevacizumab[14, 16] was reduced by administration of macrophage depletion-agent CL or galectin-3 binding inhibitor MCP. This suggests that galectin-3 may be involved in TAMs infiltration induced by anti-angiogenesis agents such as sorafenib or bevacizumab, thus a potential target in improving anti-angiogenic therapies.

In conclusion, our *in vitro* and *in vivo* investigation suggests that the upregulation of galectin-3 expression and secretion in TAMs is an important mechanism of TAMs-mediated promotion of tumor growth and metastasis in the tumor hypoxic microenvironment. The increased expression of galectin-3 is associated with an increase of intracellular ROS generation *via* activation of NF-κB nucleation. The upregulation of galectin-3 expression also enhances glucose consumption and VEGFA secretion by TAMs and promote angiogenesis under hypoxia. Moreover, galectin-3 inhibitors MCP could enhance the anti-tumor effects of anti-angiogenesis agents by inhibiting TAMs infiltration and tumor-promoting effects of TAMs *in vitro* and *in vivo*. Targeting the actions of galectin-3 in TAMs may therefore be a potential therapeutic strategy for cancer treatment.

Acknowledgements

This work was supported by the National Science Foundation of China Grants [81373450], Key Research and Development Program of Shandong Province [2017CXGC1401], The Natural Science-Crossing Disciplinary Cultivation Project of Shandong University [2017JC004] and Major Basic Research Projects of Shandong Province [ZR2018ZC0233].

Conflict of Interest

The authors declare that they have no conflict of interest.

Reference

[1] C. Ngambenjawong, H.H. Gustafson, S.H. Pun, Progress in tumor-associated macrophage (TAM)-targeted therapeutics, Adv Drug Deliver Rev 114 (2017) 206-221. Https://doi.org/10.1016/j.addr.2017.04.010

[2] M. Yang, D. McKay, J.W. Pollard, C.E. Lewis, Diverse functions of macrophages in different tumor microenvironments, Cancer Res 78(19) (2018) 5492-5503. Https://doi.org/10.1158/0008-5472.CAN-18-1367

[3] N.C. Henderson, T. Sethi, The regulation of inflammation by galectin-3, Immunol Rev 230(1) (2009) 160-171. Https://doi.org/10.1111/j.1600-065X.2009. 00794.x

[4] J.T. de Oliveira, C. Ribeiro, R. Barros, C. Gomes, A.J. de Matos, C.A. Reis, G.R. Rutteman, F. Gärtner, Hypoxia up-regulates galectin-3 in mammary tumor progression and metastasis, PLoS One 10(7) (2015) e0134458. Https://doi.org/10.1371/journal.po-ne.0134458

[5] Y. Kataoka, Y. Ohshio, T. Igarashi, K. Teramoto, J. Hanaoka, Hypoxia promotes tumor invasion via upregulation of galectin-3 in human lung cancer, Cancer Sci; 2018; 3 (11):07030-5774. Https://doi.org/ 10.3892/or.2018.6915

[6] J. Zheng, W. Lu, C. Wang, Y. Xing, X. Chen, Z. Ai, Galectin-3 induced by hypoxia promotes cell migration in thyroid cancer cells, Oncotarget 8(60) (2017) 101475. Https://doi.org/10.18632/oncotarget.21135

[7] A. Romero, H.-J. Gabius, Galectin-3: is this member of a large family of multifunctional

lectins (already) a therapeutic target? Expert Opin Ther Tar 23(10) (2019) 819-828. Https://doi.org/10.1080/14728222.2019.1675638

[8] P.P. Ruvolo, Galectin 3 as a guardian of the tumor microenvironment, BBA-Mol Cell Res 1863(3) (2016) 427-437. Https://doi.org/10.1016/j.bbamcr.2015.08.008

[9] P. Gao, P.G. Gibson, K.J. Baines, I.A. Yang, J.W. Upham, P.N. Reynolds, S. Hodge, A.L. James, C. Jenkins, M.J. Peters, Anti-inflammatory deficiencies in neutrophilic asthma: reduced galectin-3 and IL-1RA/IL-1, Resp Res 16(1) (2015) 5. Https://doi. org/10.1186/s12931-014-0163-5

[10] N.G. Frangogiannis, Galectin-3 in the fibrotic response: Cellular targets and molecular mechanisms, World J Gastro Oncol 258 (2018) 226-227. Https://doi.org/10.1016/j.ijcard.2018.01.128

[11] L.-G. Yu, Circulating galectin-3 in the bloodstream: An emerging promoter of cancer metastasis, World J Gastrointest Oncol.2(4) (2010) 177-80. Https://doi.org/10.4251/wjgo.v2.i4.177.

[12] N.C. Henderson, A.C. Mackinnon, S.L. Farnworth, T. Kipari, C. Haslett, J.P. Iredale, F.-T. Liu, J. Hughes, T. Sethi, Galectin-3 expression and secretion links macrophages to the promotion of renal fibrosis, Am J Pathol 172(2) (2008) 288-298. Https://doi.org/10.2353/ajpath.2008.070726

[13] W.-H. Kim, J.W. Lee, Y.H. Suh, H.J. Lee, S.H. Lee, Y.K. Oh, B. Gao, M.H. Jung, AICAR potentiates ROS production induced by chronic high glucose: Roles of AMPK in pancreatic T-cell apoptosis, Cell Signal 19(4) (2007) 791-805. Https://doi.org/-10.1016/j.cellsig.2006.10.004

[14] X. Hou, J. Song, X.-N. Li, L. Zhang, X. Wang, L. Chen, Y.H. Shen, Metformin reduces intracellular reactive oxygen species levels by upregulating expression of the antioxidant

thioredoxin via the AMPK-FOXO3 pathway, BiochemBioph Res Co 396(2) (2010) 199-205. Https://doi.org/10.1016/j.bbrc.2010.04.017

[15] S. Zeisberger, B. Odermatt, C. Marty, K. Ballmer-Hofer, R. Schwendener, Clodronate-liposome-mediated depletion of tumour-associated macrophages: a new and highly effective antiangiogenic therapy approach, Brit J Cancer 95(3) (2006) 272-281. Https://doi.org/10.1038/sj.bjc.6603240

[16] B.A. Castro, P. Flanigan, A. Jahangiri, D. Hoffman, W. Chen, R. Kuang, M. De Lay, G. Yagnik, J.R. Wagner, S. Mascharak, Macrophage migration inhibitory factor downregulation: a novel mechanism of resistance to anti-angiogenic therapy, Oncogene 36(26) (2017) 3749-3759. Https://doi.org/10.1038/onc.2017.1

[17] M.A. Cannarile, M. Weisser, W. Jacob, A.-M. Jegg, C.H. Ries, Dominik, Colony-stimulating factor 1 receptor (CSF1R) inhibitors in cancer therapy, J Immunother Cancer 5(1) (2017) 53. Https://doi.org/10.1186/s40425-017-0257-y

[18] J. Dumic, S. Dabelic, Galectin-3: an open-ended story, BBBA-Gen Subjects 1760(4) (2006) 616-635. Https://doi.org/10.1016/j.bbagen.2005.12.020

[19] S.N. dos Santos, H. Sheldon, J.X. Pereira, C. Paluch, E.M. Bridges, A.L. Harris, E.S. Bernardes, Galectin-3 acts as an angiogenic switch to induce tumor angiogenesis via Jagged-1/Notch activation, Oncotarget 8(30) (2017) 49484. Https://doi.org/10.18632/oncotarget.17718

[20] L. Wang, X.-L. Guo, Molecular regulation of galectin-3 expression and therapeutic implication in cancer progression, Biomed Pharm 78 (2016) 165-171. Https://doi.org/-10.1016/j.biopha.2016.01.014

[21] Y.-H. Lin, C.-H. Chou, X.-M. Wu, Y.-Y. Chang, C.-S. Hung, Y.-H. Chen, Y.-L. Tzeng, V.-

C. Wu, Y.-L. Ho, F.-J. Hsieh, Aldosterone induced galectin-3 secretion in vitro and in vivo: from cells to humans, PLoS One 9(9) (2014) e95254. Https://doi.org/10.1371/journal.pone.0095254

[22] G.-Y. Liou, P. Storz, Reactive oxygen species in cancer, Free radical research 44(5) (2010) 479-496. Https://doi.org/10.3109/10715761003667554

[23] L.B. Sullivan, N.S. Chandel, Mitochondrial reactive oxygen species and cancer, Cancer Metab 2(1) (2014) 17. Https://doi.org/10.1371/journal.pone.0033411

[24] R.P. Nishanth, R.G. Jyotsna, J.J. Schlager, S.M. Hussain, P. Reddanna, Inflammatory responses of RAW 264.7 macrophages upon exposure to nanoparticles: role of ROS-NF-κB signaling pathway, Nanotoxicology 5(4) (2011) 502-516. Https://doi.org/10.3109/17435390.2010.541604

[25] I. Jackson, I. Jackson, I. Batinic-Haberle, P. Sonveaux, M. Dewhirst, Z. Vujaskovic, ROS production and angiogenic regulation by macrophages in response to heat therapy, Int J Hyperther 22(4) (2006) 263-273. Https://doi.org/10.1080/02656730600594027

[26] Y. Zeng, K.G. Danielson, T.J. Albert, I.M. Shapiro, M.V. Risbud, HIF-1α is a regulator of galectin-3 expression in the intervertebral disc, J Bone Miner Res 22(12) (2007) 1851-1861. Https://doi.org/10.1080/02656730600594027

[27] S. Dabelic, M. Flogel, J. Dumic, Effects of aspirin and indomethacin on galectin-3, Croat Chem Acta 78(3) (2005) 433. Https://doi.org/10.1210/jcem-43-1- 107

[28] J.T. de Oliveira, R. Barros, C. Gomes, A.J. de Matos, C.A. Reis, G.R. Rutteman, Hypoxia up-regulates galectin-3 in mammary tumor progression and metastasis, PLoSOne 10(7) (2015). Https://doi.org/10.1371/journal.pone.0134458

[29] G. Hossein, S. Halvaei, Y. Heidarian, M. Hassani, H. Hosseini, N. Naderi, S. Sheikh

Hassani, Pectasol-C Modified Citrus Pectin targets Galectin-3-induced STAT3 activation and synergize paclitaxel cytotoxic effect on ovarian cancer spheroids, Cancer Med 8(9) (2019) 4315-4329. Https://doi.org/10.1002/cam4.2334

[30] T. Fang, D.-D. Liu, H.-M. Ning, D. Liu, J.-Y. Sun, X.-J. Huang, Y. Dong, M.-y. Geng, S.-f. Yun, J. Yan, Modified citrus pectin inhibited bladder tumor growth through downregulation of galectin-3, Acta Pharmacol Sin 39(12) (2018) 1885-1893. Https://doi.org/10.1210/jcem-43-1-107

[31] W. Zhang, X.-D. Zhu, H.-C. Sun, Y.-Q. Xiong, P.-Y. Zhuang, H.-X. Xu, L.-Q. Kong, L. Wang, W.-Z. Wu, Z.-Y. Tang, Depletion of tumor-associated macrophages enhances the effect of sorafenib in metastatic liver cancer models by antimetastatic and antiangiogenic effects, Clin Canc Res 16(13) (2010) 3420-3430. Https://doi.org/-10.1158/1078-0432.CCR-09-290

584

585 **Figure legends**

586 **Fig. 1. TAMs promote proliferation, invasion and migration of MDA-MB-231, and tube**
587 **formation of HUVECs under hypoxia.** (A) Expressions of M2 markers CD163 and CD68 on
588 the surface of THP-1, M2 and TAM cells were analyzed by flow cytometry. (B) M2 markers
589 (IL-1R and IL-10) and M1 markers (NOS2 and IL-12) in the THP-1, M2 and TAMs were
590 measured by RT-PCR. (C) Representative images (magnification, 200×, bar = 100 μm) show
591 tube structures of HUVECs in responses to CM of M2 or TAMs in hypoxia for 6 h. (D)
592 Following treatment with CM of M2 or TAMs for 24 h, cell proliferation of MDA-MB-231 was
593 determined by MTT assay. (E) After THP-1 cells were differentiated into M2 or TAMs and co-
594 cultured with MDA-MB-231 cells in 1% O_2 environment for 24 h, invasion or migration of
595 MDA-MB-231 cells in trans-wells were determined. Data are presented as the means ± S.E.M.
596 from three separate experiments. $^{*}P< 0.05$, $^{**}P<0.01$, v.s. Control group.

597 **Fig. 2. Hypoxia induces the expression and secretion of galectin-3 by TAMs.** Galectin-3
598 expression at protein (A) and mRNA (B) levels in M2 and TAMs after treatment of the cells
599 with sodium dithionite or cultured in 1% O_2 was determined by Western blot or RT-PCR. (C)
600 Effect of hypoxia on galectin-3 secretion from M2 or TAMs was determined by ELISA. (D)
601 Confocal microscopy images of galectin-3 localization in TAMs after treatment of the cells with
602 1% O_2 for 24 h (magnification, 600×, bar = 33 μm). (E) Immunohistochemical staining of
603 tumors from the 4T1-luc orthotopic syngeneic mouse model with antibodies against
604 Hypoxyprobe, and galectin-3 (magnification, 100×, bar = 400 μm). Data are presented as the
605 means ± S.E.M. from three separate experiments. $^{*}P< 0.05$, $^{**}P<0.01$, v.s. Control group

606 **Fig. 3. TAMs-mediated expression and secretion of galectin-3 under hypoxia promote**

migration/invasion of breast cancer cells. The migration and invasion of MDA-MB-231 cell were determined in transwell after co-incubation with M2 (A), or TAMs (B) pre-treated with siGal-3, 10 mM β-lactose or 0.1% MCP (C) for 24 h in hypoxia (magnification, 200×, bar = 100 μm). (C)The migration and invasion of MDA-MB-231 cell were determined in transwell after co-incubation with M2, or TAMs pre-treated with MCP for 24 h in hypoxia (magnification, 200×, bar = 100 μm). (D) Migration and invasion of MDA-MB-231cells were determined in transwells after co-incubation with M2 or TAMs pretreated with siGal-3 for 24 h in normoxia. (E) Cell proliferation of MDA-MB-231 after 24 h treatment with CM of TAMs in exposure to siGal-3 under hypoxia was determined by MTT assay. (F) Survival of M2 or TAMs in cell response to treatment of galectin-3 siRNA in hypoxia for 24 h was determined by MTT assay. (G) Glucose consumption of M2 or TAMs treated with or without galectin-3 siRNA under normoxia and hypoxia was determined by Glucose Assay. (H, I) Secretion of galectin-3 and VEGFA by M2 or TAMs treated without or with galectin-3 siRNA were measured by ELISA. Data are presented as the means ± S.E.M. from three separate experiments. $^{*}P<0.05$, $^{**}P<0.01$ v.s. Scrambled siRNA; $^{\Delta}P<0.05$, $^{\Delta\Delta}P<0.01$ v.s. β-lactose + galectin-3; $^{\#}P<0.05$, $^{\#\#}P<0.01$ v.s. Hypoxia.

Fig. 4. Galectin-3 secretion by TAMs promotes angiogenesis and vascular mimicry under hypoxia. Representative images (magnification, 200×, bar = 100 μm) show vascular mimicry of MDA-MB-231 cells (A) or tube formation of HUVECs (B) after 6 h incubation of the cells with CM from hypoxic or normoxia (C) TAMs. (D) Representative images show HUVECs tube structures after 6 h incubation with MCP or CM from hypoxic TAMs. (E) Cell proliferation of HUVECs after 24 h treatment with CM of TAMs in exposure to siGal-3 under hypoxia was determined by MTT assay. (F) Cell migration and invasion of HUVECs was determined in transwell in cell co-culture with TAMs treated with siGal-3 or/and β-lactose for 24 h under

hypoxia (magnification, 200×, bar = 100 μm). Data are presented as the means ± S.E.M. from three separate experiments. $^{*}P<0.05$, $^{**}P<0.01$, v.s. Scrambled siRNA; $^{\Delta}P<0.05$, $^{\Delta\Delta}P<0.01$ v.s. β-lactose + galectin-3.

Fig. 5. Upregulation of galectin-3 in TAMs under hypoxia is dependent on NF-κB *via* ROS. (A) Expression of galectin-3, AMPK, PI3K and HIF-1α in hypoxic TAMs were analyzed by Western blot. (B) The level of NF-κB in hypoxic TAMs were assessed by immunofluorescence (magnification, 100×, bar = 200 μm). (C) Effects of PDTC (10 μM, pretreatment for 1 h), LY294002 (0.5 μM, pretreatment for 1 h), compound C (4 μM, pretreatment for 1 h) and 2ME2 (10 μM, pretreatment for 0.5 h) on mRNA expression of galectin-3 in TAMs under hypoxia or normoxia were determined by RT-PCR. (D, E) The protein expression of galectin-3 in TAMs in hypoxia pretreated with metformin (5 mM) or AICAR (1 mM) for 1h was assessed by Western blot. (F) Level of ROS in hypoxic TAMs pretreated with PDTC, LY294002, compound C, 2ME2 and NAC were analyzed by immunofluorescence (magnification, 100×, bar = 200 μm). (G) Effects of rosup (50 mg/ml, pretreatment for 1 h), NAC (10 nM, pretreatment for 1 h) on galectin-3 mRNA expression in TAMs were analyzed by RT-PCR. (H) NF-κB in TAMs pretreated with LY294002, compound C, 2ME2 and NAC was analyzed by immunofluorescence. Data are presented as the means ± S.E.M. from three separate experiments. $^{*}P<0.05$, $^{**}P<0.01$ v.s. Normoxia control; $^{\#}P<0.05$, $^{\#\#}P<0.01$ v.s. Hypoxia control.

Fig. 6. Hypoxia induces galectin-3 secretion and that promotes tumor metastasis and angiogenesis *in vivo*. Balb/c mice were injected with 5×10^5 4T1-luc cells into the mammary fat pad under #3 mammary gland. Mice were daily treated with 8% O_2 for 6 h, with or without intratumoral injection of 2% MCP (0.5 μL/g/day) for 21 days. (A, B) Expressions of CD68, galectin-3 and CD31 in tumor tissues were analyzed by immunofluorescence. (B)Expression of CD31 in tumor tissues was analyzed by Immunohistochemistry. (C) Lung metastasis of 4T1-

breast cancer cells from mammary fat pad was recorded using an *in vivo* imaging system (n = 5). (D) Serum galectin-3 level in mice was detected by ELISA. All data are presented as means ± SD, n = 5, $^{*}P<0.05$ v.s. Normoxia control mice; $^{\#}P<0.05$ v.s. Hypoxia control mice.

Fig. 7. Galectin-3 is involved in hypoxia aggravation and macrophage infiltration induced by antiangiogenic agents. (A) Lung metastasis in nude mice of breast cancer was established by intravenous injection of MDA-MB-231-luc cells by tail vein. The lung metastasis was assessed using an *in vivo* imaging system. (B) Serum concentration of galectin-3 in the mice was measured by ELISA. (C, D) Balb/c mice were injected with 5×10^5 4T1-luc cells into the mammary fat pad under #3 mammary gland. The body weight (C) and tumor volume (D) of mice were recorded every 3 days for 21 days. (E) Serum concentration of galectin-3 in mice was measured by ELISA. (F, G) The orthotopic growth and lung metastasis was analyzed using an *in vivo* imaging system (n = 5). Hypoxia area and macrophage infiltration (H) and galectin-3 expression (I) in tumor sections were analyzed by immunofluorescence. (J) Expression of CD31 in tumor tissues was analyzed by Immunohistochemistry. All data are presented as means ± SD, n = 5, $^{*}P<0.05$, $^{**}P<0.01$ v.s. Hypoxia control group; $^{\#}P<0.05$, $^{\#\#}P<0.01$ v.s. Sorafenib group or Bevacizumab group.

Fig 1

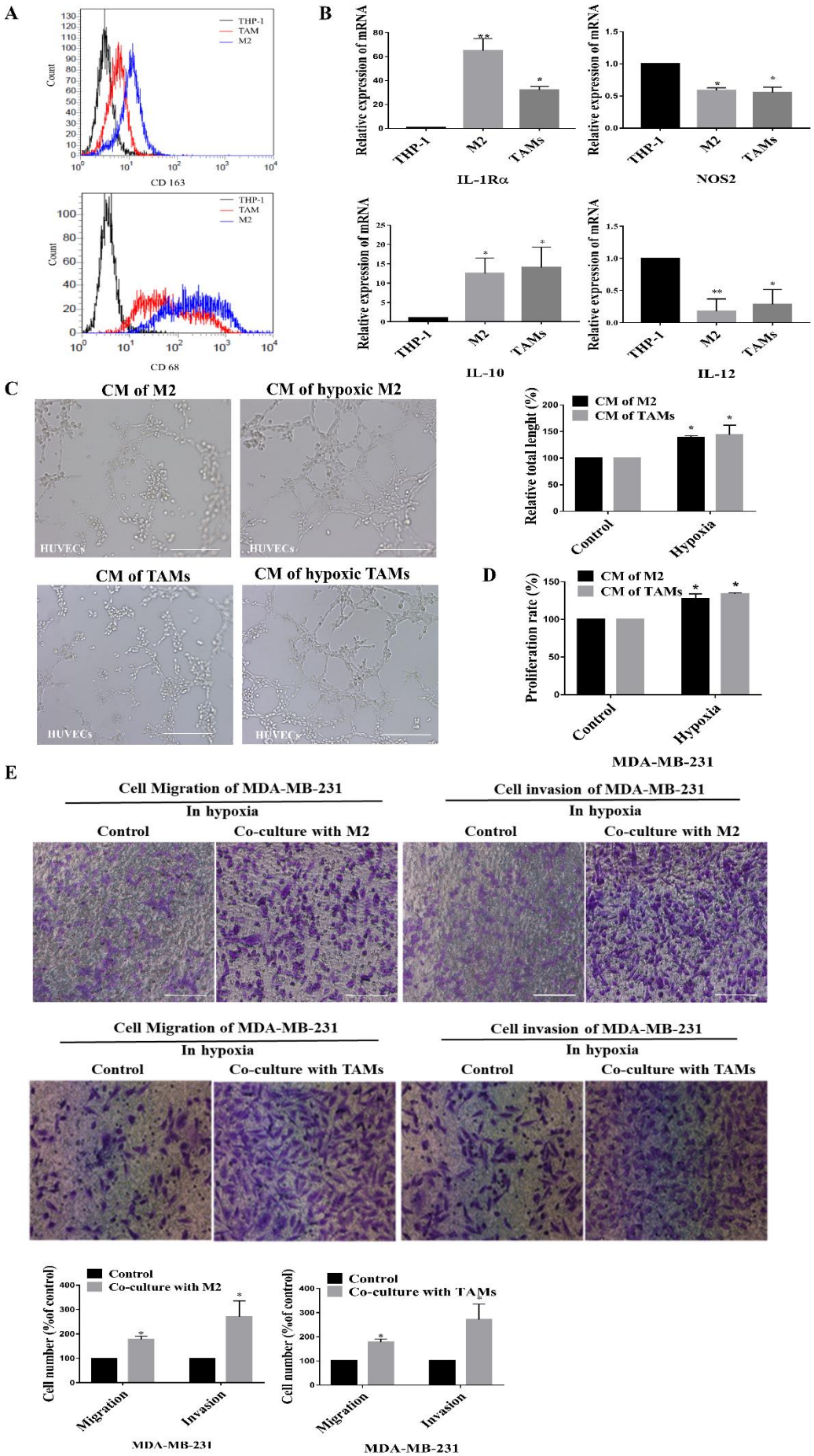
A
THP-1
TAM
M2
Count
CD 163
CD 68
B
Relative expression of mRNA
IL-1Rα
NOS2
IL-10
IL-12
THP-1
M2
TAMs
C
CM of M2
CM of hypoxic M2
CM of TAMs
CM of hypoxic TAMs
HUVECs
Relative total lenght (%)
Control
Hypoxia
D
Proliferation rate (%)
MDA-MB-231
E
Cell Migration of MDA-MB-231
Cell invasion of MDA-MB-231
In hypoxia
Control
Co-culture with M2
Co-culture with TAMs
Cell number (%of control)
Migration
Invasion

674 Fig 2

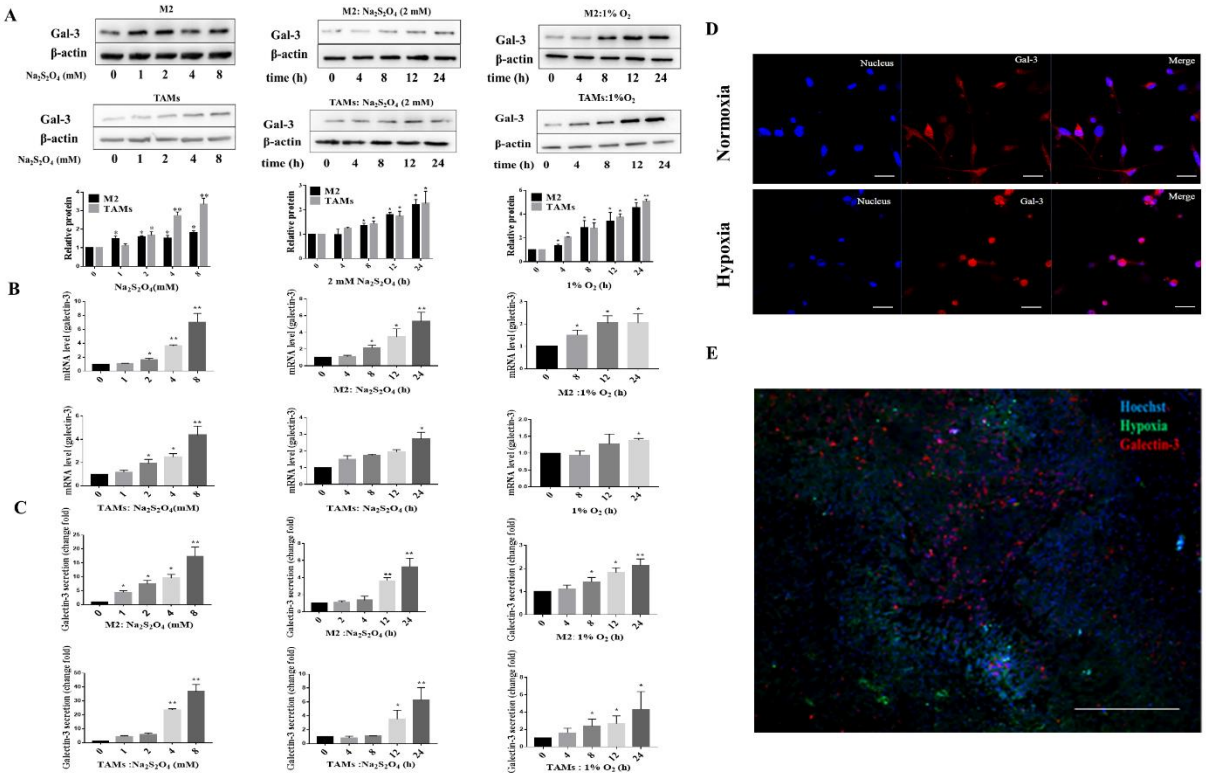

675

676 Fig 3

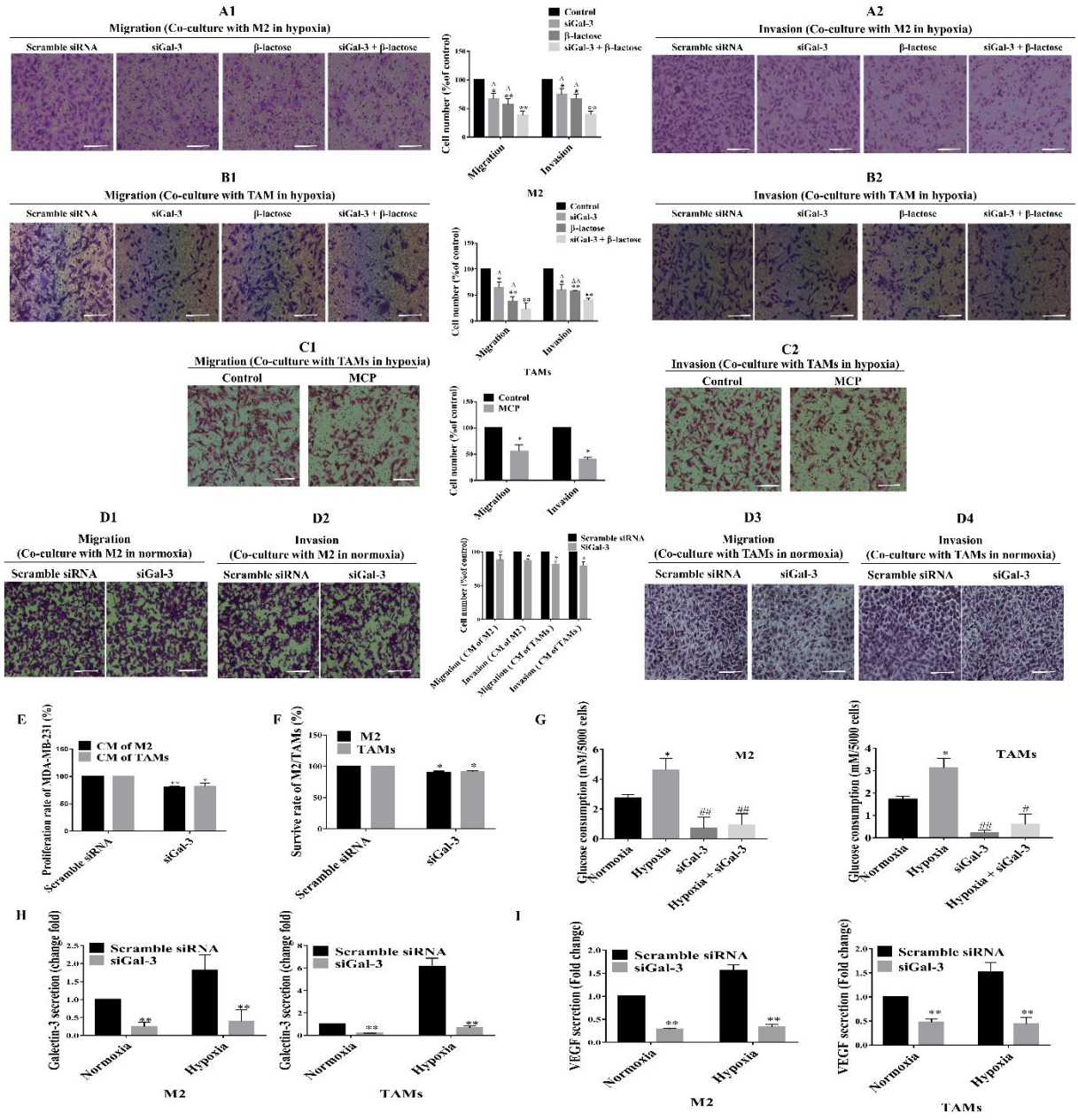
A1
Migration (Co-culture with M2 in hypoxia)
Scramble siRNA
siGal-3
β-lactose
siGal-3 + β-lactose
Control
siGal-3
β-lactose
siGal-3 + β-lactose
Cell number (%of control)
Migration
Invasion
A2
Invasion (Co-culture with M2 in hypoxia)
B1
Migration (Co-culture with TAM in hypoxia)
M2
TAMs
B2
Invasion (Co-culture with TAM in hypoxia)
C1
Migration (Co-culture with TAMs in hypoxia)
Control
MCP
C2
Invasion (Co-culture with TAMs in hypoxia)
D1
Migration
(Co-culture with M2 in normoxia)
D2
Invasion
(Co-culture with M2 in normoxia)
D3
Migration
(Co-culture with TAMs in normoxia)
D4
Invasion
(Co-culture with TAMs in normoxia)
Migration (CM of M2)
Invasion (CM of M2)
Migration (CM of TAMs)
Invasion (CM of TAMs)
E
Proliferation rate of MDA-MB-231 (%)
CM of M2
CM of TAMs
F
Survive rate of M2/TAMs (%)
G
Glucose consumption (mM/5000 cells)
Normoxia
Hypoxia
siGal-3
Hypoxia + siGal-3
H
Galectin-3 secretion (change fold)
I
VEGF secretion (Fold change)

677

678 Fig 4

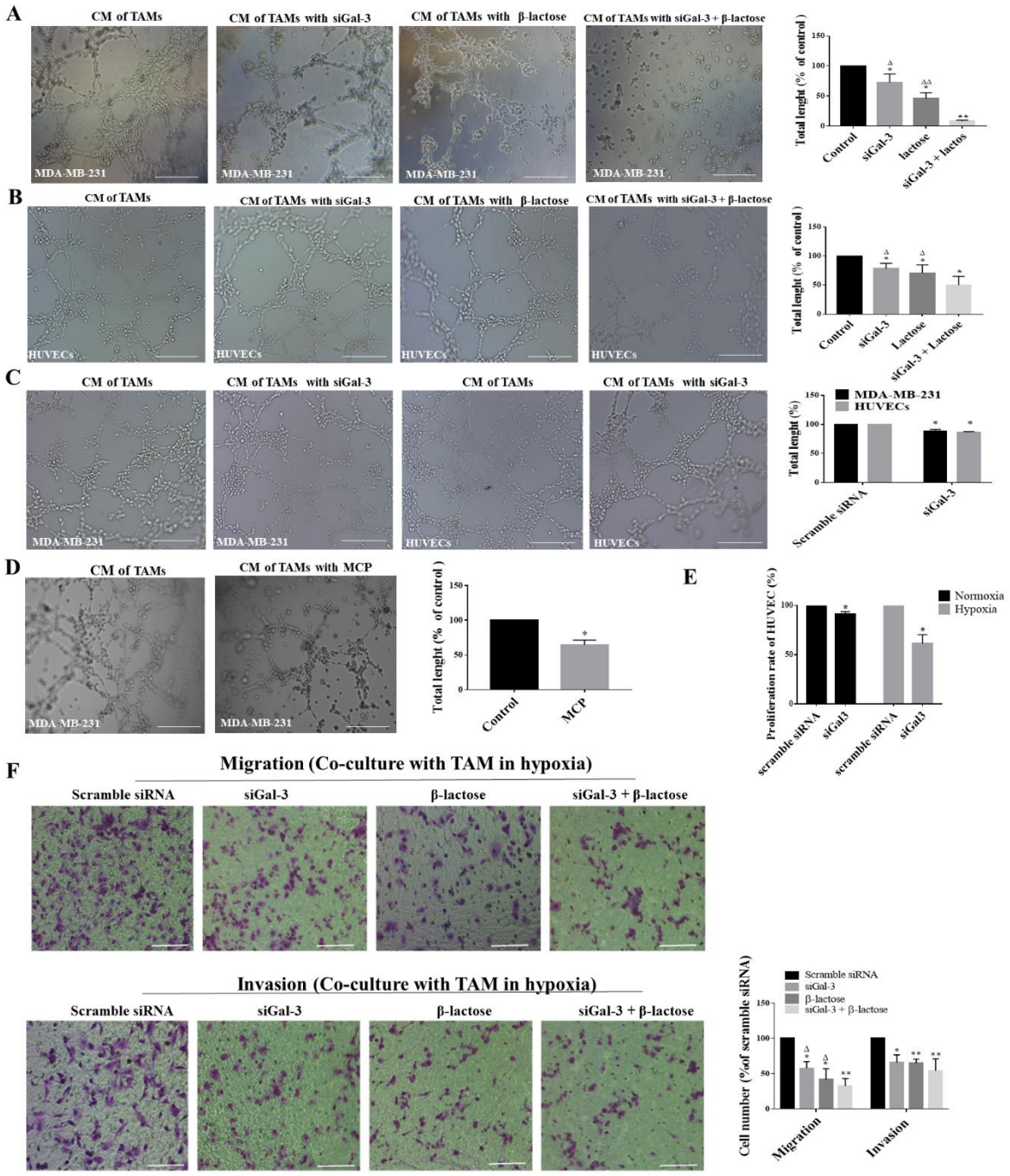

679

680

681 Fig 5

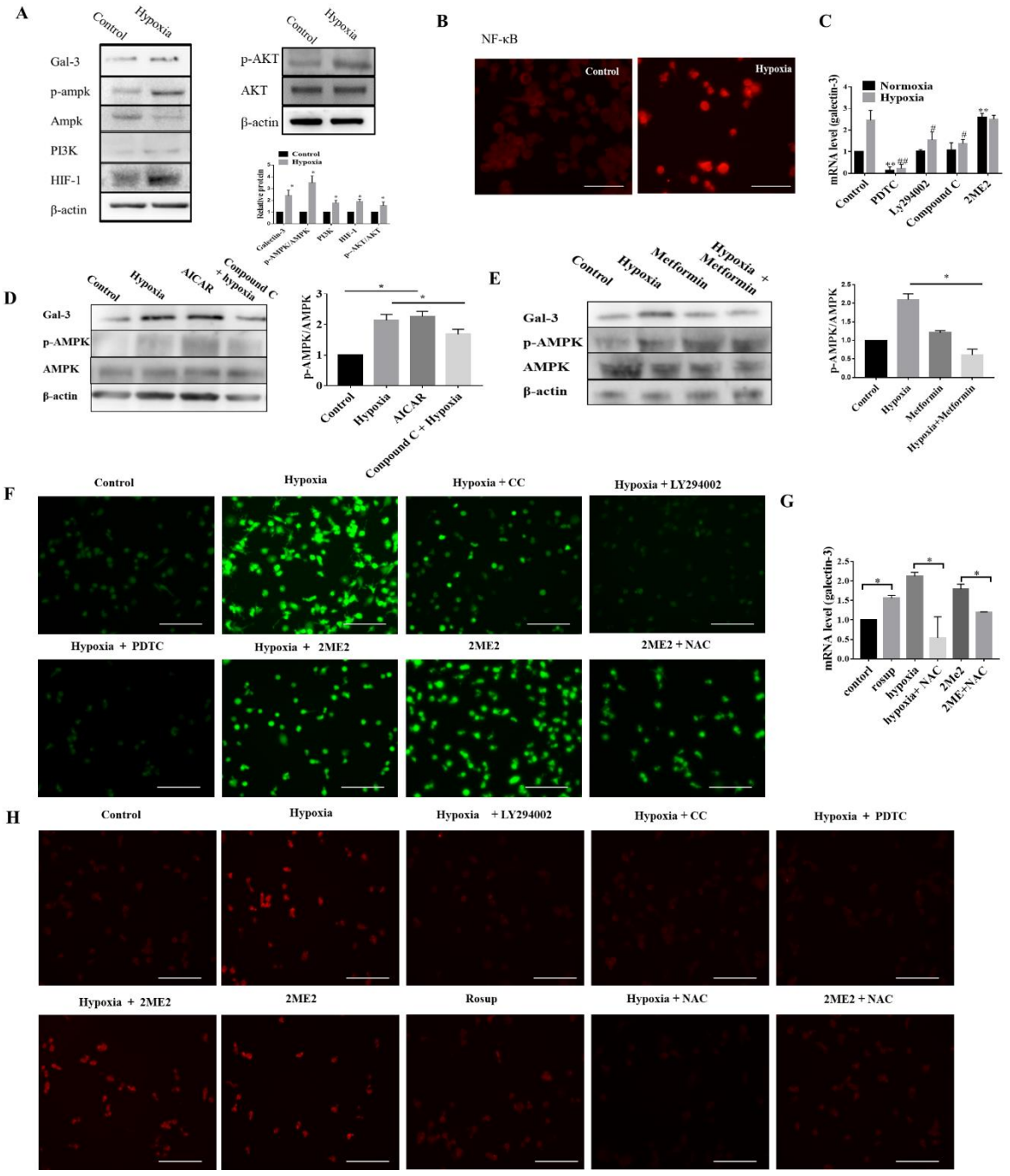
A
Control
Hypoxia
Gal-3
p-ampk
Ampk
PI3K
HIF-1
β-actin
p-AKT
AKT
β-actin
B
NF-κB
Control
Hypoxia
C
Normoxia
Hypoxia
mRNA level (galectin-3)
Control
PDTC
Ly294002
Compound C
2ME2
D
Control
Hypoxia
AICAR
Compound C + hypoxia
Gal-3
p-AMPK
AMPK
β-actin
p-AMPK/AMPK
E
Control
Hypoxia
Metformin
Hypoxia + Metformin
Gal-3
p-AMPK
AMPK
β-actin
p-AMPK/AMPK
Control
Hypoxia
Metformin
Hypoxia+Metformin
F
Control
Hypoxia
Hypoxia + CC
Hypoxia + LY294002
Hypoxia + PDTC
Hypoxia + 2ME2
2ME2
2ME2 + NAC
G
mRNA level (galectin-3)
contor1
rosup
hypoxia
hypoxia+ NAC
2Me2
2ME2+NAC
H
Control
Hypoxia
Hypoxia + LY294002
Hypoxia + CC
Hypoxia + PDTC
Hypoxia + 2ME2
2ME2
Rosup
Hypoxia + NAC
2ME2 + NAC

682

683 Fig 6

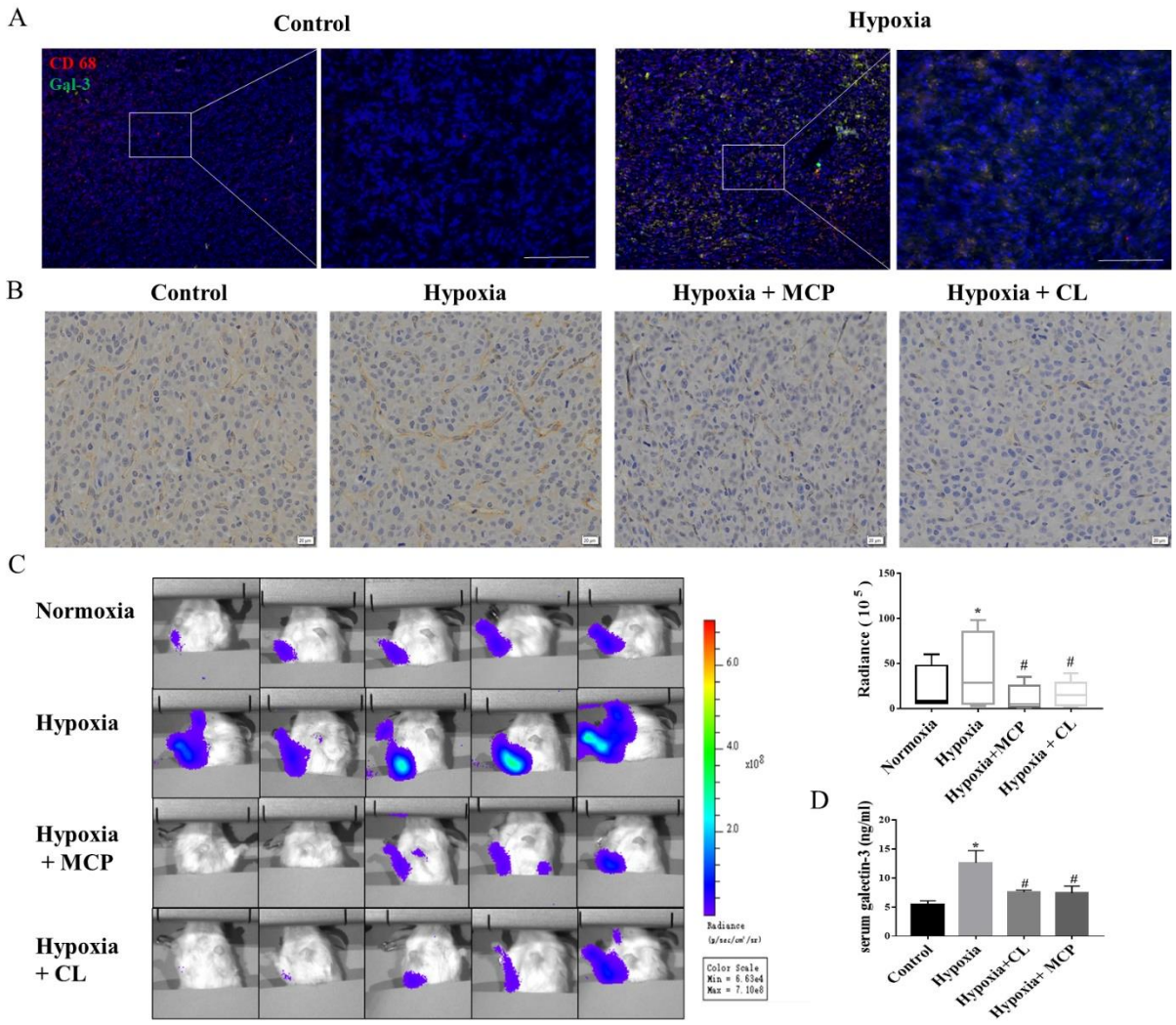
A
Control
Hypoxia
CD 68
Gal-3
B
Control
Hypoxia
Hypoxia + MCP
Hypoxia + CL
C
Normoxia
Hypoxia
Hypoxia + MCP
Hypoxia + CL
6.0
4.0
x10^8
2.0
Radiance (p/sec/cm²/sr)
Color Scale
Min = 6.63e4
Max = 7.10e8
D
Radiance (10^5)
150
100
50
0
*
#
#
Normoxia
Hypoxia
Hypoxia+MCP
Hypoxia + CL
serum galectin-3 (ng/ml)
20
15
10
5
0
*
#
#
Control
Hypoxia
Hypoxia+CL
Hypoxia+ MCP

684

685 Fig 7

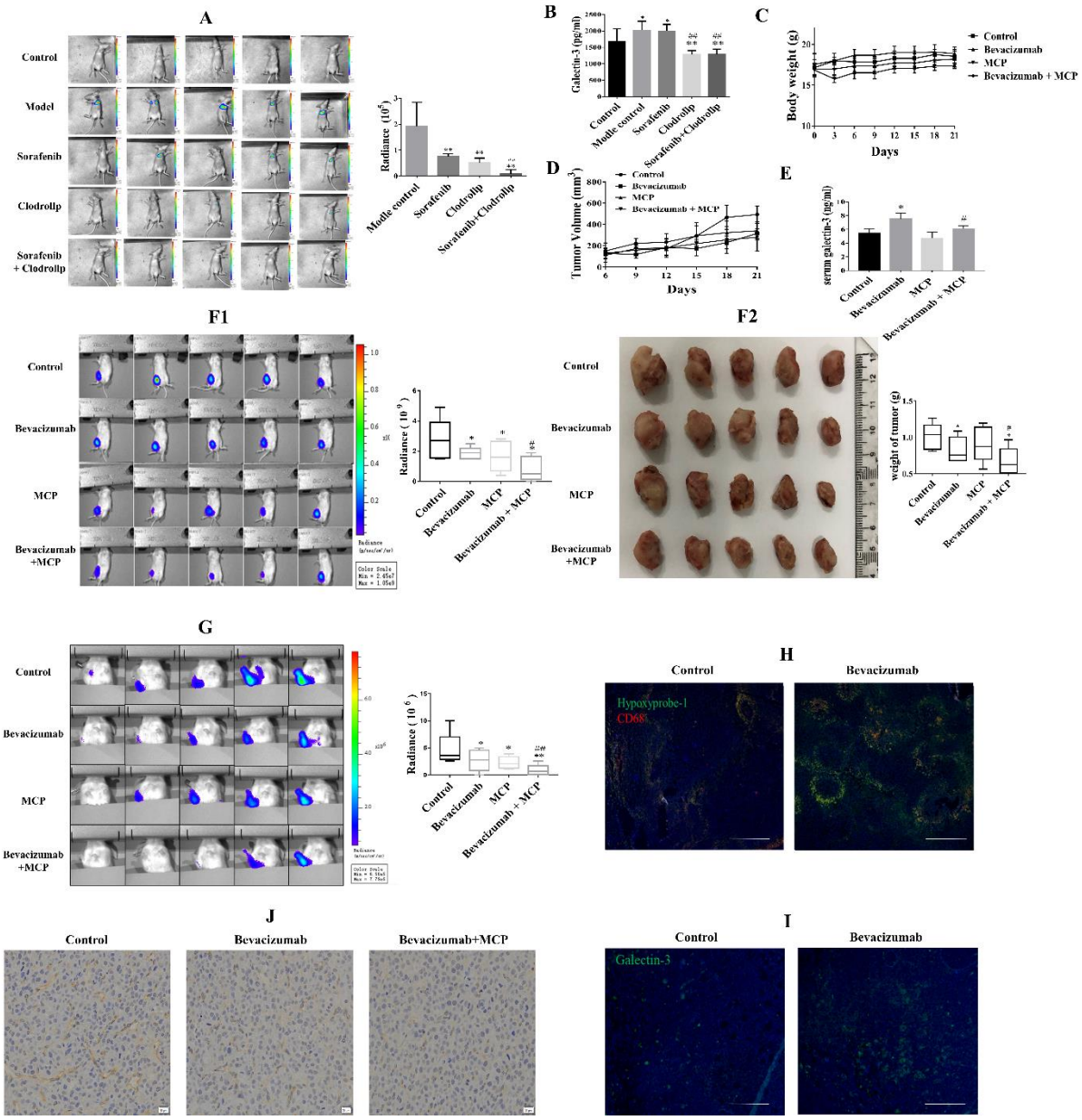

Graphic abstract

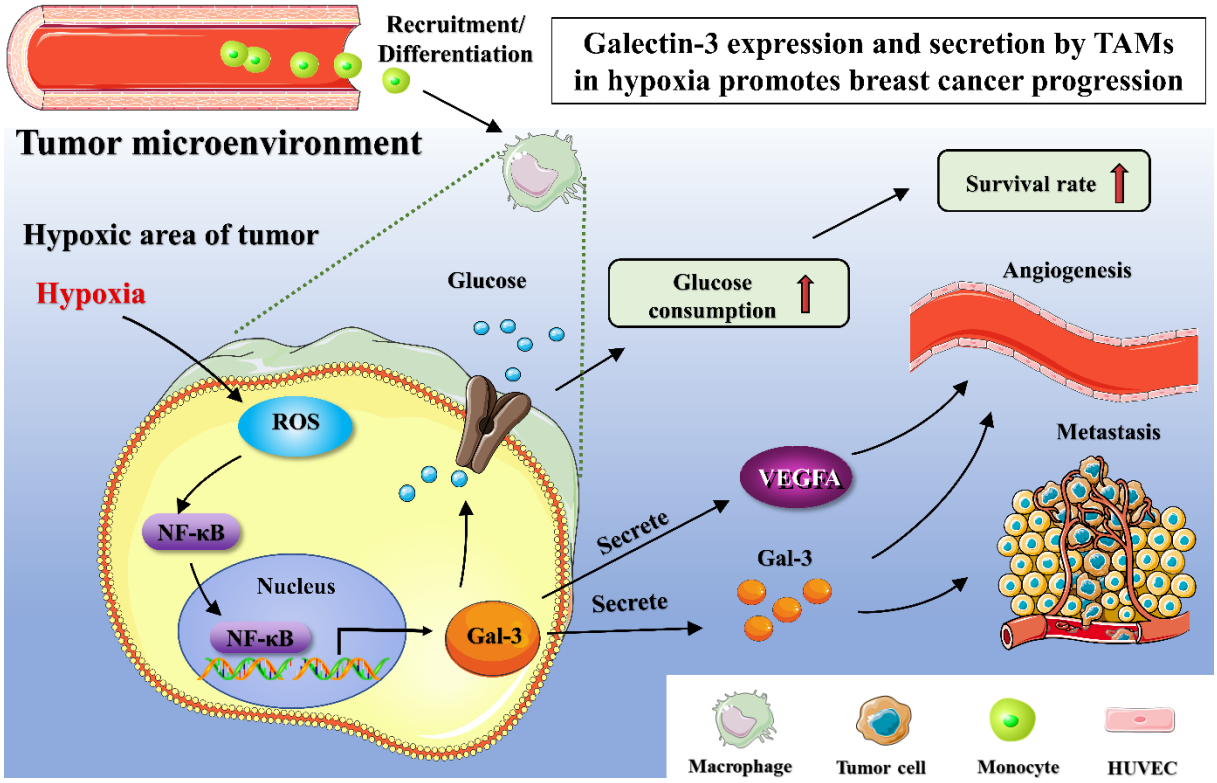
Recruitment/
Differentiation
Galectin-3 expression and secretion by TAMs
in hypoxia promotes breast cancer progression
Tumor microenvironment
Hypoxic area of tumor
Hypoxia
Glucose
Glucose
consumption
Survival rate
Angiogenesis
ROS
NF-κB
Nucleus
NF-κB
Gal-3
Secrete
Secrete
VEGFA
Gal-3
Metastasis
Macrophage
Tumor cell
Monocyte
HUVEC

688